Desalination and Water Treatment
www.deswater.com
doi:10.5004/dwt.2017.20422

72 (2017) 249–265
April

Enhanced degradation of ternary dye effluent by developed bacterial consortium with RSM optimization, ANN modeling and toxicity evaluation

Priya Banerjee[a], Shramana Roy Barman[a], Dolanchapa Sikdar[b], Uttariya Roy[b], Aniruddha Mukhopadhayay[a], Papita Das[b,*]

[a]*Department of Environmental Science, University of Calcutta, 35, Ballygunge Circular Road, Kolkata – 700 019, India, email: prya_bnrje@yahoo.com (P. Banerjee), shromonaroybarman123@gmail.com (S. Roy Barman), am_cuenvs@yahoo.co.in (A. Mukhopadhayay)*
[b]*Department of Chemical Engineering, Jadavpur University, 188, Raja S.C. Mullick Road, Kolkata - 700 032, India, email: dolanchapa30@gmail.com (D. Sikdar), uttariyar@gmail.com (U. Roy), papitasaha@gmail.com (P. Das)*

Received 8 July 2016; Accepted 9 December 2016

ABSTRACT

The present study investigated the simultaneous removal of Safranin (SA), Crystal violet (CV) and Methylene blue (MB) by a bacterial consortium consisting of *Dietzia* sp., *Bacillus* sp. and *Pseudomonus mendocina* in batch reactors. The effect of experimental parameters like initial dye concentration, solution pH, salinity and temperature on the process of biodegradation was also studied. On optimization of ternary dye degradation using both RSM (CCD) and ANN on a comparative scale, RSM was found to be a more suitable approach. Application of RSM optimised conditions resulted in 99.87, 98.74 and 97.57% decolorization of SA CV and MB respectively. Effect of dye exposure on bacterial cells was investigated using atomic force microscopy (AFM). The untreated and treated samples were analysed using Fourier transform infrared (FTIR) spectroscopy for characterization of metabolites formed due to dye degradation. Phytotoxicity assay with *Cicer arietinum* showed that seedlings exposed to untreated effluents showed significantly impaired growth, biochemical and enzyme (oxidative stress response and detoxification) parameters in comparison to those exposed to treated effluents which in turn were at par with control levels. The results obtained denoted efficient detoxification of ternary dye effluent by the selected bacterial consortium and hence proved its applicability for treatment of real effluent.

Keywords: Ternary azo dye system; Biodegradation; Response surface methodology; Artificial neural network; *Cicer arietinum;* Phytotoxicity assay

1. Introduction

Azo dyes appear in extensive amounts in almost all types of effluents and thereby severely contaminate ecosystems and water bodies adjacent to their points of discharge [1]. Of an approximate seven hundred thousand tonnes of ten thousand different commercial dyes globally produced each year [2], the textile industry alone has been reported responsible for an annual discharge of nearly a hundred and forty six thousand tonnes of mixed dyes along with its effluents [1]. A few other noteworthy contributors of dye pollutants include industries producing cosmetics, leather, paint, paper, plastics, pharmaceuticals, etc. Synthetic dyes applied for industrial processes often bear azo, nitro and/or sulfo groups which often render these dyes and their degraded products biorecalcitrant in nature [1]. Many dyes have been assessed to exert carcinogenic and mutagenic effects as well [3,4]. Safranin, Crystal violet and Methylene blue are few

*Corresponding author.

examples of basic azine dyes widely used for industrial purposes [1,2,5]. Inspite of implementing diverse technologies, a cost effective and widely applicable approach for treatment of dye-rich wastewater is yet to be achieved.

Detrimental effects exerted on the environment due to dye pollutants necessitate the application of environmentally benign treatment technologies that may be implemented on a wide scale in a cost and energy efficient manner. Conventional physical and chemical treatment technologies reported till date incur huge cost as well as operational glitches and often terminate in incomplete dye degradation with successive CO_2 production [6]. Application of biological oxidation was only found to ascertain complete degradation of dye moieties in solution [6]. Previous studies have reported acceptable and efficient aerobic treatment of dye rich effluents using algae, bacteria, fungi and yeasts with a primary focus on fungal (mainly using ligninolytic enzymes of fungal origin) degradation [7]. However, dye removal by bacterial species has less reported in comparison to other micro-organisms [7]. In this regard, application of microbial consortia may be considered more advantageous over single microbial specie as in the former case, higher enzymatic capacity is obtained for acting on diverse pollutants [8]. Besides, toxic intermediate metabolites produced as a result of bacterial degradation are converted to harmless end products by co-metabolism processes [9]. However, optimization of experimental conditions for achieving maximum detoxification of mixed dyes still remains a challenge thereby hindering their wide scale application for real effluent treatment [10].

In most of the existing literature, diverse groups of microorganisms (actinomycetes, bacteria, fungi, etc) have been reported as capable of degrading azo dyes [11]. However, assorted dye mixtures and influence of vital experimental parameters and their interaction soften limit the application of microorganisms for treatment of industrial effluents. Previous studies have mostly investigated effect of individual experimental parameters as it is tedious, time consuming and complicated to execute the huge number of experiments required for determining their combined effects [11]. Hence, in recent years, different statistical analogies are being implemented for process optimization and investigation of parameter interaction in highly reduced number of experiments thereby reducing time required and cost incurred. Response surface methodology (RSM) and Artificial neural network (ANN) are two such widely implemented tools of process optimization.

In this study, a ternary dye system consisting of Safranin (SA), Crystal violet (CV) and Methylene blue (MB) was subjected to treatment using a bacterial consortium consisting of two isolated species i.e. *Dietzia* sp., *Bacillus* sp. and *Pseudomonas mendocina* (MTCC11808) for aerobic degradation. All selected species were previously reported capable of unary dye degradation [11,12] and therefore tested for their applicability in mixed dye scenario. The interactions of the experimental parameters like initial dye concentration, solution pH, salinity and temperature guiding this process were optimized using both the Central composite design (CCD) feature of Response surface methodology (RSM) and Artificial neural network (ANN). The significance of the tested RSM and ANN models was calculated with analysis of variance (ANOVA). The experimental combinations suggested by RSM were further used for training and validation of different ANN models. Theoretically predicted and experimentally obtained results from RSM (CCD) and ANN analysis were compared for identifying the most appropriate tool for optimization. Bacterial cells were imaged using atomic force microscopy (AFM) both pre and post treatment to analyze the effect of dyes on the same. Fourier transform infrared (FTIR) spectroscopy of untreated and treated samples confirmed degradation of dyes in solution. A further comparative analysis of phytotoxicity induced by both untreated and treated samples on chick pea (*Cicer arietinum*) seedlings was also carried out.

2. Experimental methodology

2.1. Materials and instruments

SA ($C_{20}H_{19}ClN_4$; λ_{max} = 516nm), CV ($C_{25}N_3H_{30}Cl$; λ_{max} = 589 nm) and MB ($C_{16}H_{18}ClN_3S$; λ_{max} = 630 nm) of commercial grade was purchased and used as procured. All other chemicals used for this study were purchased from Merck, India (analytical grade). Stock solutions were prepared in distilled water with 100 mg L^{-1} of dyes and further diluted with distilled water to obtain working solutions of desired dye concentrations. All through this study, the solution pH was adjusted with addition of 0.1 N HCl or 0.1 M NaOH as and when required.

Solution pH was measured using a pH meter (Extech D0700, India). Initial and final dye concentrations in solution were determined with an UV-VIS spectrophotometer (Perkin Elmer λ 35, USA) using a quartz cuvette (optical path = 1 cm). Changes in surface morphology of bacterial cells were visualised with the aid of AFM (Innova, Veeco, Bruker AXS Pte Ltd., Massachusetts). Infrared spectra of untreated and treated mixed dye samples were derived with a FTIR spectrometer (JascoFTIR-6300, Japan) in the KBr pellet method.

2.2. Isolation and culture conditions of selected strains

The individual strains forming the consortium were selected on the basis of their ability of rapid dye degradation as reported in previous studies. The isolation procedures of pure cultures of *Dietzia* sp. PD1 have been reported elsewhere [1]. *Bacillus* sp. PD5 was isolated and identified for this study from a water source adjacent to a local textile dyeing unit in the same procedure as reported previously [1]. The GenBank accession number for *Bacillus* sp. PD5 was KU901698. The pure culture of *Pseudomonas mendocina* (MTCC11808) was purchased from Microbial Type Culture Collection and Gene Bank, Institute of Microbial Technology, Chandigarh, India.

All selected strains were separately maintained on agar slants of composition reported earlier [13] with a subculture prepared every two months. For obtaining inoculums, loopful of each isolate was added to 50 mL of an agar-less broth of the same composition (growth media) and incubated for a day at 30 ±2°C with a constant agitation of 120 rpm. For assessing their dye degrading ability, 1 mL of each inoculum type was simultaneously added to 97 mL of basal salt media (BSM) solutions prepared as per Tony et al. [14] and supplemented with SA, CV and MB (prepared in 1:1:1 ratio where concentration of each dye varied from 15–75 mg L^{-1})

as sources of carbon and energy. After five transfers of basal medium, the stabilized co-cultures obtained were stored at –80°C and sub-cultured in basal media for further analysis.

2.3. Biodegradation studies

Batch studies were continued for 6 days. All experiments were carried out in Erlenmeyer flasks of 250 ml capacity. For investigating effect of initial dye concentration on the biodegradation process, 5 mL of pre grown bacterial consortium cultures (O.D. < 800) was added to 95 mL of ternary dye solutions (prepared in 1:1:1 ratio) prepared in BSM with concentration of each dye ranging from 15–75 mg L^{-1}. Effect of variable solution pH (6–10), salt concentration (0–10 g L^{-1}) and temperature (25–40°C) on biodegradation of ternary dye solution by prepared co-culture was also determined. All flasks were incubated in a rotary shaker (120 rpm). Throughout each experiment, samples were collected every six hours, centrifuged (8000 rpm, 15 min) and analyzed for residual dye concentration using a UV-VIS spectrophotometer at respective wavelength of each dye.

Rate of dye degradation was expressed as percentage (%) decolorization calculated using the following equation (1):

$$\%\text{Decolorization} = \frac{\text{Initial dye concentration} - \text{Final dye concentration}}{\text{Initial dye concentration}} \times 100 \quad (1)$$

All experiments were repeated thrice for minimization of handling error and results were represented as Mean ± SD of three consecutive estimations.

2.4. Optimization using CCD feature of RSM

In this study, process optimization and inter-parameter interactions affecting the process of ternary dye biodegradation were addressed by a mathematical and statistical based tool known as RSM. In this approach, 3D plots portraying a response surface able to identify optimum experimental conditions favoring the concerned process are developed with an appropriate model signified by analysis of variance (ANOVA). For optimization and better understanding of ternary dye biodegradation by prepared bacterial consortium, a three level (low, central and high) six factor (including initial SA, CV and MB concentrations, solution pH, salinity and time) model was designed with the Central composite design (CCD) feature of RSM using Design Expert, Version 7.0 Minneapolis, USA. This model in turn suggested a total of 86 experiments with 10 replications around the center. The selected parameters (factors) along with their respective units, ranges and levels as well as the suggested experiments have been given in Supplementary Table 1.

As indicated by the RSM analysis, the empirical relationship connecting the six independent variables (factors) was guided by the quadratic polynomial equation described as follows:

$$Y = m_0 + \sum_{i=1}^{k=5} m_i x_i + \sum_{i=1}^{k=5} \sum_{j=1}^{k=5} m_{ij} x_i x_j + \sum_{i=1}^{k=5} m_{ii} x_i^2 + E \quad (2)$$

where Y = response (dependent variable), m_0= constant coefficient, m_a ($a = i, j, ij$, etc. representing regression coefficients of linear, quadratic and interaction respectively), x_b ($b = i, j$, etc. denoting different experimental parameters respectively) and E = error.

Both predicted and experimental outputs (% Decolorization of SA, CV and MB) obtained from the 86 experiments suggested by RSM design matrix have been described in Supplementary Table 1 on a comparative scale. Optimization of the concerned process was carried out with Derringer's desirability function (DF) [15,16]. For optimization of the concerned process, the applied goals given in the menu were selected as within range and maximum respectively for factors and responses. In order to achieve maximum desirability, the initial dye concentration (for each of SA, CV and MB), solution pH, salinity and time were fixed in the range of 6.63–18.37 mg L^{-1}, 3.3–9.3, 5.54–9.45 g L^{-1} and 4–10 d respectively.

2.5. ANN modeling

Artificial Neural Network (ANN) is a type of mathematical model inspired by the biological neural schema [16]. In an ANN model, independent variables are entered as predetermined inputs that are carried forward to neurons and further transmitted by preferred activation functions (consisting of assorted feature detectors) for production of output responses in the form of dependent variables. A three layer feed forward neural model consisting of an input, a hidden and an output layer was developed in this present study with MATLAB 7 (The Mathworks Inc.; Ver. 7.0.1). Different functions like "poslin", "tansig", "satlin" and "logsig" were evaluated as transfer functions in the hidden layer. "Purelin" function was used as transfer function in the output layer. The RSM model had suggested a total of 86 experiments with 10 replications around the center. Of these 86 experiments, the 76 unique combinations were used for the training and validation of the ANN model designed and implemented in this study. Experimental parameters (initial individual dye concentration, solution pH, salinity and time) and % decolorization of each dye were chosen as the input and output of this model respectively.

The experimental data were normalized prior to being and tested with different algorithms for model validation. Of the four tested back-propagation (BP) algorithms used for training the designed model (including Levenberg-Marquardt (Trainlm), Resilient (Trainrp), Scaled conjugate gradient (Trainscg) and Gradient descent with momentum and adaptive learning rate (Traingdx)), the one with the highest coefficient of determination (R^2) was considered as best fit to the concerned process. Training of the neural networks is strongly guided by the number of neurons in the hidden layer. A higher number of neurons usually ensure a better performance of the designed model in fitting the data. However an excessive number of neurons in the hidden layer may lead to over fitting [17]. Number of neuron for the hidden layer was optimized by trial and error method. Best results were ensured by fixing the performance target and ramp.

2.6. Comparative analysis of RSM and ANN approach

The estimation capabilities of the suggested RSM and ANN techniques for ternary dye degradation by

selected bacterial consortium have been analyzed on a comparative scale as suggested previously [18]. Predicted responses of both techniques were compared to observed data obtained from 86 experiments suggested by RSM (CCD). The performance of each technique was statistically assessed by the parameters described as follows [18]:

$$R^2 = 1 - \sum_{i=1}^{n}\left(\frac{\left(Y_{i,P} - Y_{i,E}\right)^2}{\left(Y_{i,P} - Y_A\right)^2}\right) \quad (3)$$

$$RSME = \sqrt{\frac{\sum_{i=1}^{n}\left(Y_{i,P} - Y_{i,E}\right)^2}{n}} \quad (4)$$

$$MAE = \frac{\sum_{i=1}^{n}\left|Y_{i,P} - Y_{i,E}\right|}{n} \quad (5)$$

$$AAD\% = \left(\frac{1}{n}\sum_{i=1}^{n}\left(\frac{Y_{i,P} - Y_{i,E}}{Y_{i,P}}\right)\right) \times 100 \quad (6)$$

where R^2 = coefficient of determination, RSME = root mean squared error, MAE = mean absolute error, AAD = absolute average deviation, n = number of experimental data, $Y_{i,P}$, $Y_{i,E}$, and Y_A = predicted response, experimental response and average of experimental values respectively.

The percentage of total response is denoted by R^2 and estimated by least-squares regression. On the other hand AAD is a more direct approach for determining measure of deviation between predicted and experimental results. While R^2 values should be close to unity, AAD% should be as low as achievable [18]. Comparatively lower values of RSME and MAE also signify appropriateness of the technique being assessed.

2.7. AFM imaging of bacterial cells

AFM analysis is an extremely appropriate technique of visualizing bacterial samples and has been so far widely implemented for imaging and investigating other properties of bacterial cells [13]. The samples for AFM analysis do not require fixation, conductive coating or vacuum imaging there by rendering the process simple and convenient [13]. In this study, samples were prepared on freshly cleaved mica sheets by drop deposition method. 20 µL of the sample was dropped carefully on mica sheets and dried for complete removal of moisture. Tapping mode images (2D and 3D) of samples plated on mica sheets were recorded with a constant raster scanning speed (1Hz) at 300 ± 2 K and 75% RH.

2.8. FTIR analysis of treated and untreated samples

The biodegraded metabolites from samples with highest % decolorization were extracted with ethyl acetate and dried as reported earlier [19]. The product obtained and the ternary dye mixture was cast into separate pellets with potassium bromide (KBr) of FTIR grade and scanned (400–4000 cm^{-1}) with a 4 cm^{-1} resolution using an FTIR spectrometer.

2.9. Phytotoxicity analysis

Toxicity analysis of untreated and treated ternary dye solutions were carried out with gram (*Cicer arietinum*) seeds. *C. arietinum* is a protein rich pulse crop with efficient nitrogen fixing ability widely grown and consumed in the Indian subcontinent, the Mediterranean region, Ethiopian, and Mexican provinces [20]. Gram seeds used for this study were commercially obtained from a local market. Seeds of uniform dimensions were treated with 0.1% (*w*/*v*) $HgCl_2$ solution for surface sterilization for a whole minute followed by thorough rinsing (thrice) using distilled water.

2.9.1. Effect of germination and growth

A total of three experimental groups were prepared consisting of control (distilled water treated), untreated dye ternary dye solutionscontaining 15 mg L^{-1} of each dyeand biotreated dye solutions. For each treatment type, twenty five surface sterilized gram seeds were placed on a filter paper (Whatman® no. 3) in a glass Petri plate (12 cm diameter). 10 mL of each treatment was added to the Petri plate of respective treatment every 24 h. the plates were then incubated in dark at 25°C in a seed germinator (Yorco Y58765; India). Seeds developing root tips of 1 mm and higher length were considered to be germinated [21]. After initiation of germination, percentage of seeds germinated and length (in mm) of the seedling roots and shoots were measured once every 24 h for the next three days.

2.9.2. Effect on biochemical parameters

Protein estimation of root and shoot tissues of treated seedlings was carried out with folin reagent [22] while free amino acid content of the same was estimated with ninhydrin reagent [22]. Carbohydrate (soluble and insoluble) content of root and shoot tissues was determined using anthrone reagent [22]. Total amylase activity of the treated seedlings was obtained with 3, 5 dinitrosalicylic acid as described by Goswami et al. [22]. All estimations were performed using a UV-Vis spectrophotometer.

2.9.3. Oxidative stress analysis

For estimation of oxidative stress enzyme activities in treated seedlings, 100 mg of root and shoot tissues from each treatment were separately homogenized in chilled phosphate buffer (0.1 M, pH 7.0) and centrifuged (12,000 rpm, 15 min, 4°C). The supernatants were collected and stored for enzyme assays. The protein content of these samples was derived with bovine serum albumin as standard protein [21]. Oxidative stress response was determined by alterations in Guaiacol peroxidase (POD), Catalase (CAT) and Superoxide dismutase(-SOD) activities. Estimation of Glutathione peroxidase (GP_x), Glutathione-S-transferase (GST) and Glutathione reductase (GR) activities were carried out according to Banerjee et al. [10] as indicative of detoxification enzyme activities.

2.10. Statistical analysis

All experimental procedures were triplicated to reduce handling error and data were represented as Mean ± SD. Data analysis was performed using Microsoft Excel 2007 program and Origin software (version 9.1; Origin Lab Corporation, USA). Statistical calculations of RSM optimization and ANN modeling were carried out with Design Expert, Version 7.0 Minneapolis, USA and MATLAB 7 (The Mathworks Inc.; Ver. 7.0.1) respectively. Statistical significance of phytotoxicity analysis was obtained with two sample independent *t* test and one-way ANOVA using GraphPad InStat 3 (San Diego, CA, USA).

3. Results and discussion

3.1. Batch studies

3.1.1. Effect of initial dye concentration

Supplementary Fig. 1 (A, E and I) show the effect of initial dye concentration on % decolorization of SA, CV and MB respectively. In all three cases, an increase in initial dye concentration was paralleled by a decrease in % decolorization. % Decolorization was found to be highest when initial dye concentration was 15 mg L^{-1} for each dye in the mixture and was found to be 99.93, 99.20 and 99.55% for SA, CV and MB respectively. This decrease in decolorizing efficiency of the selected consortium may have resulted from toxic influence of dyes on bacterial cells or inappropriate biomass concentration in the treated solution [1].

3.1.2. Effect of solution pH

Supplementary Fig. 1 (B, F and J) denote the influence of solution pH on % decolorization of SA, CV and MB respectively. It is evident from these three figures, that, other factors remaining constant, maximum dye degradation was obtained in the range of pH 6–7. % Decolorization was also found to decrease with an increase in alkaline nature of the test solutions (pH 8–10). Alkaline medium may have hindered the transportation of dye molecules across cellular membranes thereby influencing the rate-limiting step of the biodegradation process [1].

3.1.3. Effect of salinity

Supplementary Fig. 1 (C, G and K) depict the effect of initial salt concentration on % decolorization of SA, CV and MB respectively. Results revealed that % dye decolorization had increased with a corresponding increase in salt concentration (0–7.5 g L^{-1}). Decrease in % dye decolorization with a further increase in salt concentration (10g L^{-1}) may have occurred due to detrimental impact of high salt concentration on osmotic pressure of bacterial cells which in turn may have inhibited bacterial growth causing cell death [23]. Similar results were reported by Rajeswari et al. [24]. Besides dye residues, effluents from textile and dye processing units often contain substantial concentrations of salt. Increase in % dye decolorization with a simultaneous increase in salt concentration therefore rendered the selected bacterial consortium suitable for treating real-time wastewaters.

3.1.4. Effect of temperature

Supplementary Fig. 1 (D, H and L) illustrate the effect of ambient temperature on % decolorization of SA, CV and MB respectively. Results obtained indicated highest % ternary dye decolorization at 35°C. Substantial inhibition of % decolorization at other tested temperatures may have occurred from deactivation of dye degrading enzymes or degeneration of cell viability at those temperatures [23].

3.2. Analysis of RSM (CCD) optimization

Predicted and actual results of the experiments suggested by RSM (CCD) have been presented as % SA, CV and MB removal in Supplementary Table 1. The F values for % decolorization of SA, CV and MB were found to be 763.88, 642.51 and 687.57 respectively. The large F values indicated a 0.01% chance of its occurrence due to noise. The large F values also indicated the predicted quadratic polynomial model as best fit and thereby rendered every term of the quadratic polynomial equation to be highly significant ($p < 0.0001$) at 95% confidence level. The quadratic model selected for this study was also validated by a "Lack of Fit F-value" insignificant in comparison to the pure error and probably generated by noise. The coefficient of regression, R^2 (0.9972, 9967 and 0.9969), the adjusted R^2 (0.9959, 9951 and 0.9954) and the predicted R^2 (0.9933, 9935 and 0.9938) for SA, CV and MB removal respectively were in considerable agreement and hence denoted the quadratic polynomial model as best fit amidst all other tested models for predicting the performance of the process under concern. The Adeq Precision values for simultaneous removal of ternary dyes were estimated to be 86.48, 81.29 and 84.83 for % decolorization of SA, CV and MB respectively indicating a signal adequate for navigation of the design space. The RSM (CCD) analysis therefore established that the chosen model predicted the theoretical % dye decolorization (given in Supplementary Table 1) with a semi-empirical expression based on the following equations:

$$\begin{aligned}\%\ \text{SA Removal} = {} & -127.49556 + 4.23038 * A - 1.41512 * B + 0.018122 * C + 20.56773 * D + 24.74559 * E + 5.88871 * F - 0.017287 * A * B - 4.50434E-003 * A * C + 0.044291 * A * D + 0.10809 * A * E + 0.072055 * A * F + 0.032837 * B * C + 0.057283 * B * D + 0.13503 * B * E - 0.052790 * B * F - 0.066299 * C * D - 0.032265 * C * E + 1.36501E-003 * C * F + 0.73247 * D * E + 0.17184 * D * F + 0.19322 * E * F - 0.24169 * A^2 + 2.64559E-003 * B^2 + 0.010339 * C^2 - 1.73110 * D^2 - 2.13076 * E^2 - 0.41208 * F^2 \end{aligned} \quad (7)$$

$$\begin{aligned}\%\ \text{CV Removal} = {} & -138.21985 + 4.83200 * A - 1.55720 * B - 0.42871 * C + 21.35300 * D + 24.76008 * E + 6.84089 * F - 0.034801 * A * B - 0.010578 * A * C + 0.022611 * A * D + 0.083147 * A * E + 0.097797 * A * F + 0.040371 * B * C + 0.057540 * B * D + 0.13007 * B * E - 0.054465 * B * F - 0.069716 * C * D - 6.66806E-003 * C * E - 1.18108E-003 * C * F + 0.72983 * D * E + 0.23860 * D * F + 0.18518 * E * F - 0.24917 * A^2 + 0.013275 * B^2 + 0.019408 * C^2 - 1.79258 * D^2 - 2.11479 * E^2 - 0.50086 * F^2 \end{aligned} \quad (8)$$

$$\% \text{ MB Removal} = -146.84704 + 5.48089 * A - 1.72402 * B - 0.34889 * C + 22.08931 * D + 25.67441 * E + 5.96881 * F - 0.030700 * A * B - 0.013871 * A * C + 6.53142E\text{-}003 * A * D + 0.092727 * A * E + 0.099520 * A * F + 0.048019 * B * C + 0.056653 * B * D + 0.13393 * B * E - 0.040040 * B * F - 0.095575 * C * D - 0.049697 * C * E + 9.70032E\text{-}003 * C * F + 0.76828 * D * E + 0.29083 * D * F + 0.21254 * E * F - 0.27509 * A^2 + 7.89312E - 003 * B^2 + 0.029957 * C^2 - 1.85715 * D^2 - 2.17433 * E^2 - 0.49760 * F^2 \quad (9)$$

where A–F denoted initial SA conc. (mg L^{-1}), initial CV conc. (mg L^{-1}), initial MB conc. (mg L^{-1}), initial solution pH, initial solution salinity (g L^{-1})and time (days) respectively.

Results obtained showed good accord between model predicted and experimentally recorded data. The significant inter-parameter interactions ($p < 0.0001$, as per ANOVA analysis) guiding the simultaneous degradation of SA, CV and MB have been presented as 3D contour plots in Figs. 1–3 and described below.

3.2.1. Interaction of solution pH and initial dye concentration

The 3D surface plots shown in Figs. 1A, 2A and 3A show the effect of variations in initial solution pH and initial dye concentration on % decolorization of SA, CV and MB respectively. Both independent variables were seen to impose a strong influence on percentage removal of ternary dyes. A maximum % dye decolorization of 98.99, 96.13 and 94.24 of SA, CV and MB respectively was recorded with initial concentration of 12.50 mg L^{-1} for each dye at an initial solution pH of 6.3. A gradual decline in % dye decolorization was also noted with further rise in both parameters. An increase in alkaline nature of surrounding medium coupled with toxic influence of dyes on bacterial cells may be considered responsible for the aforesaid reduction in dye decolorizing efficiency of selected consortium. Similar results were also reported by Das et al. [1] in a previous study for separate bacterial degradation of congo red and indigo carmine.

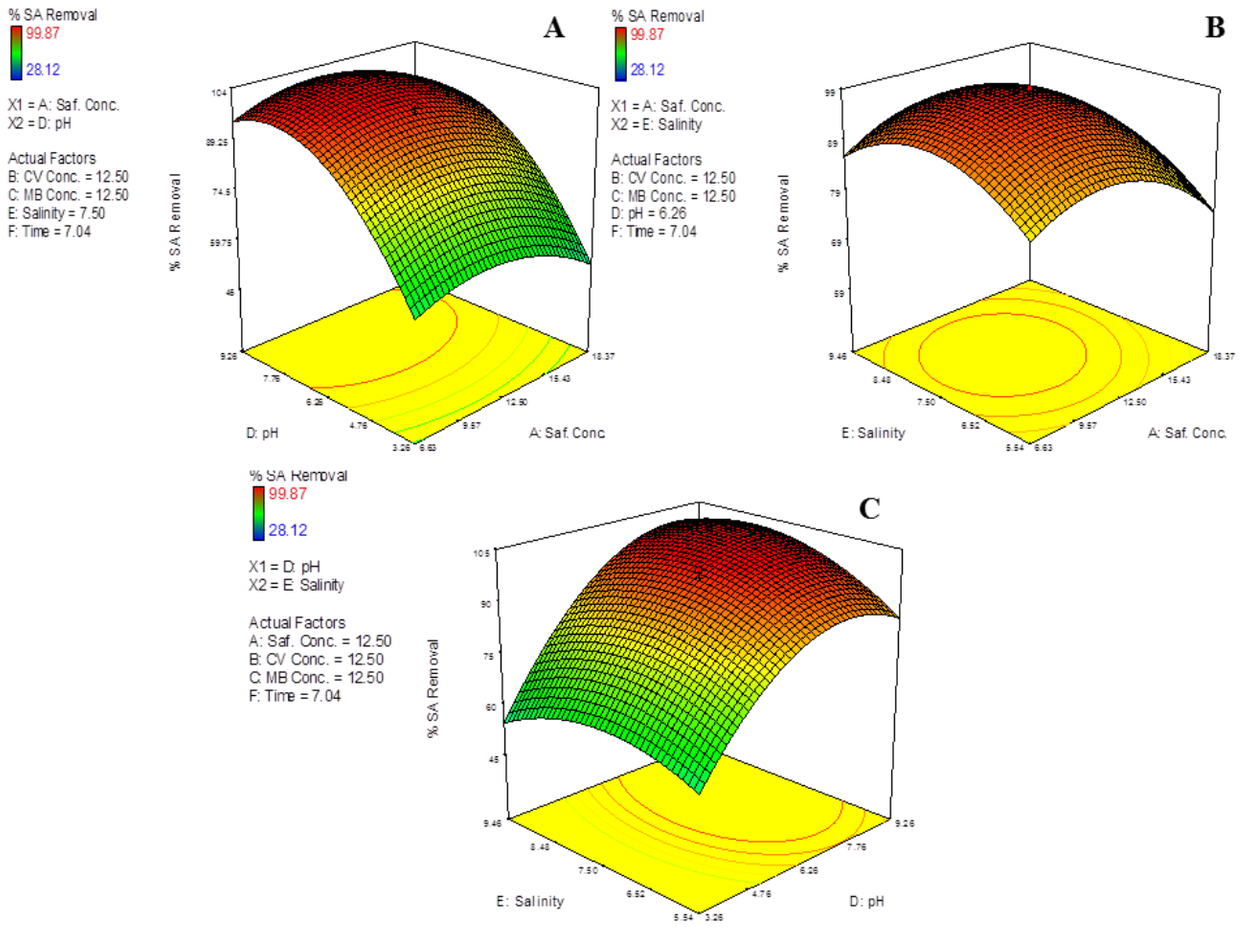

Fig. 1. 3D plots showing effect of independent variables on simultaneous % Decolorization of SA using selected bacterial consortium as determined from RSM analysis. A, B and C illustrate interactions of varying solution pH and initial dye concentration, salt concentration and initial dye concentration and solution pH and salt concentration on SA degradation respectively.

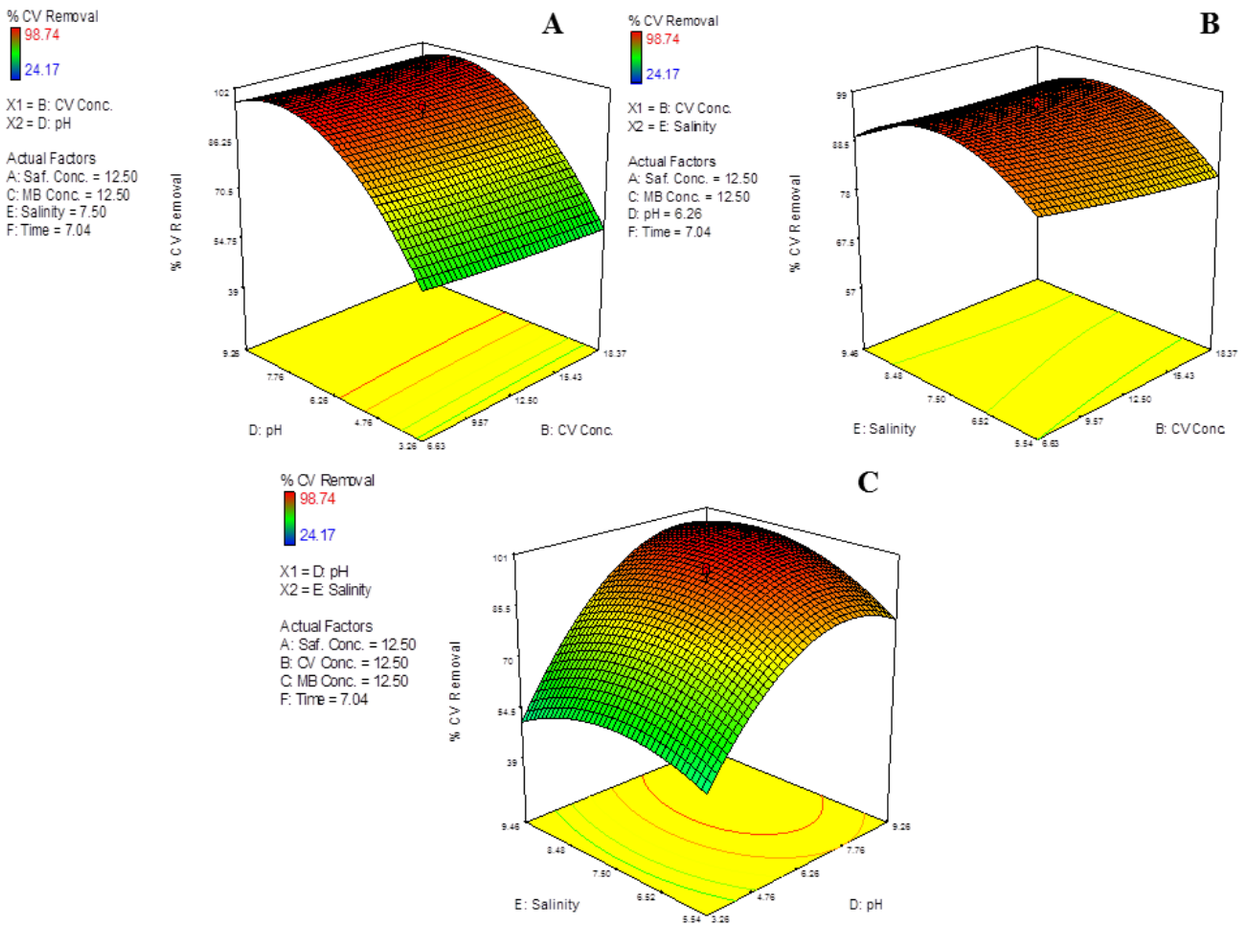

Fig. 2. 3D plots showing effect of independent variables on simultaneous % Decolorization of CV using selected bacterial consortium as determined from RSM analysis. A, B and C illustrate interactions of varying solution pH and initial dye concentration, salt concentration and initial dye concentration and solution pH and salt concentration on CV degradation respectively.

3.2.2. Interaction of salinity and initial dye concentration

Figs. 1B, 2B and 3B show 3D surface plots depicting effect of variable salinity and initial dye concentration on percentage removal of SA, CV and MB respectively. % removal of dyes increased with an increase in both parameters and was found to be the highest at an initial concentration of 12.50 mg L^{-1} for each dye and a salinity of 7.50 g L^{-1}. Further rise in salinity and dye concentration was paralleled with a decrease in dye decolorization which may have resulted from inhibition of bacterial growth at higher values of the concerned parameters.

3.2.3. Interaction of solution pH and salinity

The effect of simultaneous variations in solution pH and salinity on % removal of SA, CV and MB have been illustrated in the 3D surface plots shown in Figs. 1C, 2C and 3C respectively. Results revealed that a subsequent rise in pH (6.3–9.3) resulted in decolorization efficiency of bacterial consortium to occur over a wider range of salinity (7.5–9.5 g L^{-1}). Efficient decolorization in presence of high salt concentration rendered the consortium highly suitable for treatment of wastewaters bearing high quantities of salt. Similar results were reported by Asad et al. [25] and Kolekar et al. [26].

3.2.4. Derringer's desirability function (DF)

Comparative analysis of the theoretically predicted and experimentally obtained responses of RSM (CCD) analysis revealed a deviation of 0.69, 0.72 and 0.76% for SA, CV and MB % removal respectively. According to Derringer's DF, the highest desirability (0.986) was recorded when a ternary dye mixture with initial SA, CV and MB concentration of 13.52, 18.30 and 18.37 mg L^{-1} correspondingly was treated with the selected bacterial consortium for 10 days at an initial solution pH and of 6.5 an initial salt concentration of 9.46 g L^{-1}. Application of these optimum experimental conditions resulted in 99.87, 97.42 and 95.65 % SA, CV and MB removal respectively.

3.3. Analysis of ANN modeling

The schematic representation of the multilayer feed forward neural network model used in this study has been

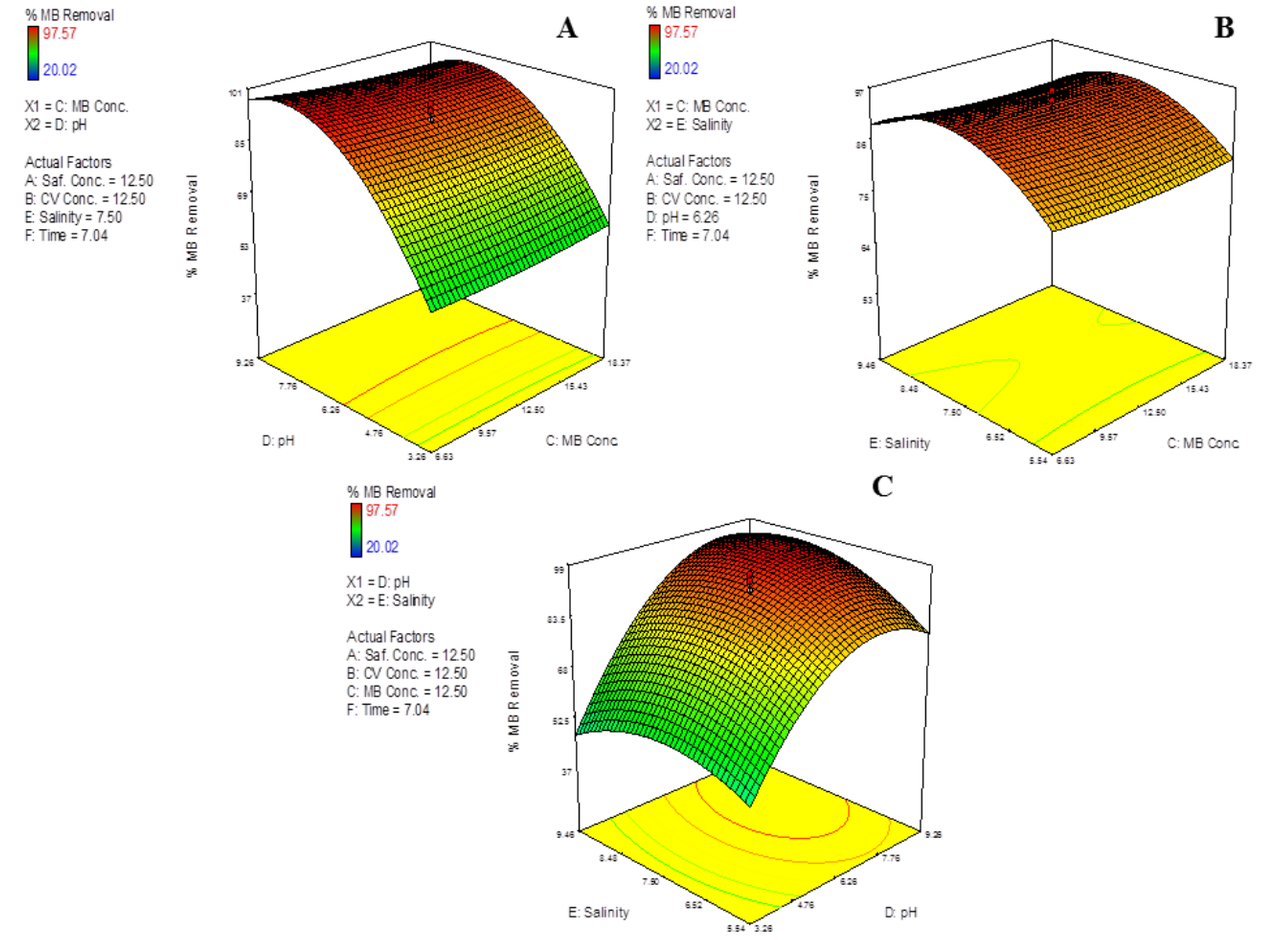

Fig. 3. 3D plots showing effect of independent variables on simultaneous % Decolorization of MB using selected bacterial consortium as determined from RSM analysis. A, B and C illustrate interactions of varying solution pH and initial dye concentration, salt concentration and initial dye concentration and solution pH and salt concentration on MB degradation respectively.

shown in Fig. 4A. Based on RSM analysis, 6 neurons were chosen as input layers and 3 were chosen as output layers. The maximum number of epochs (training cycles) was chosen by a trial and error approach. Performance goal and minimum performance gradient were set so as to ensure a model with good performance. The original data set (comprising of 85 data points) was divided into three subsets (as 3:1:1) – training (45 data points), validation (15 data points) and test sets (15 data points). The split of data into training, validation and test subsets was carried out to estimate the performance of the neural network for prediction of "unseen" data that were not used for training. In this way, the generalization capability of ANN model was assessed. One experimental point representing low, medium and high value ranges were compared with the recorded data for test and validation of the network model.

The theoretically predicted responses obtained from ANN modeling has been shown in Supplementary Table 1. The highest correlation values obtained for Resilient back propagation (Trainrp) algorithm was found to be 0.987, 0.952 and 0.942 for SA, CV and MB removal respectively rendering the same best fit for modeling experimental data obtained amidst other tested models. The theoretically predicted responses obtained from ANN modeling has been shown in Supplementary Table 1. However, ANN predicted data was of inferior fit in comparison to that obtained from RSM analysis, proving the latter to be a better tool for guiding the concerned process.

3.4. Comparative analysis of RSM and ANN approach

The comparative results of the assessed statistical parameters (i.e. R^2, RMSE, AAD and MAE) of applied RSM (CCD) and ANN model has been given in Supplementary Table 1. As suggested by Azad et al. [18], the relatively higher R^2 and lower RMSE, AAD and MAE values for RSM established the same as a more appropriate approach over ANN analysis. The RSM and ANN analysis plots showing theoretically predicted vs. experimentally obtained results have been shown in Fig. 4B and 4C respectively. Results revealed higher deviation between experimentally obtained data and ANN predicted ones in comparison to

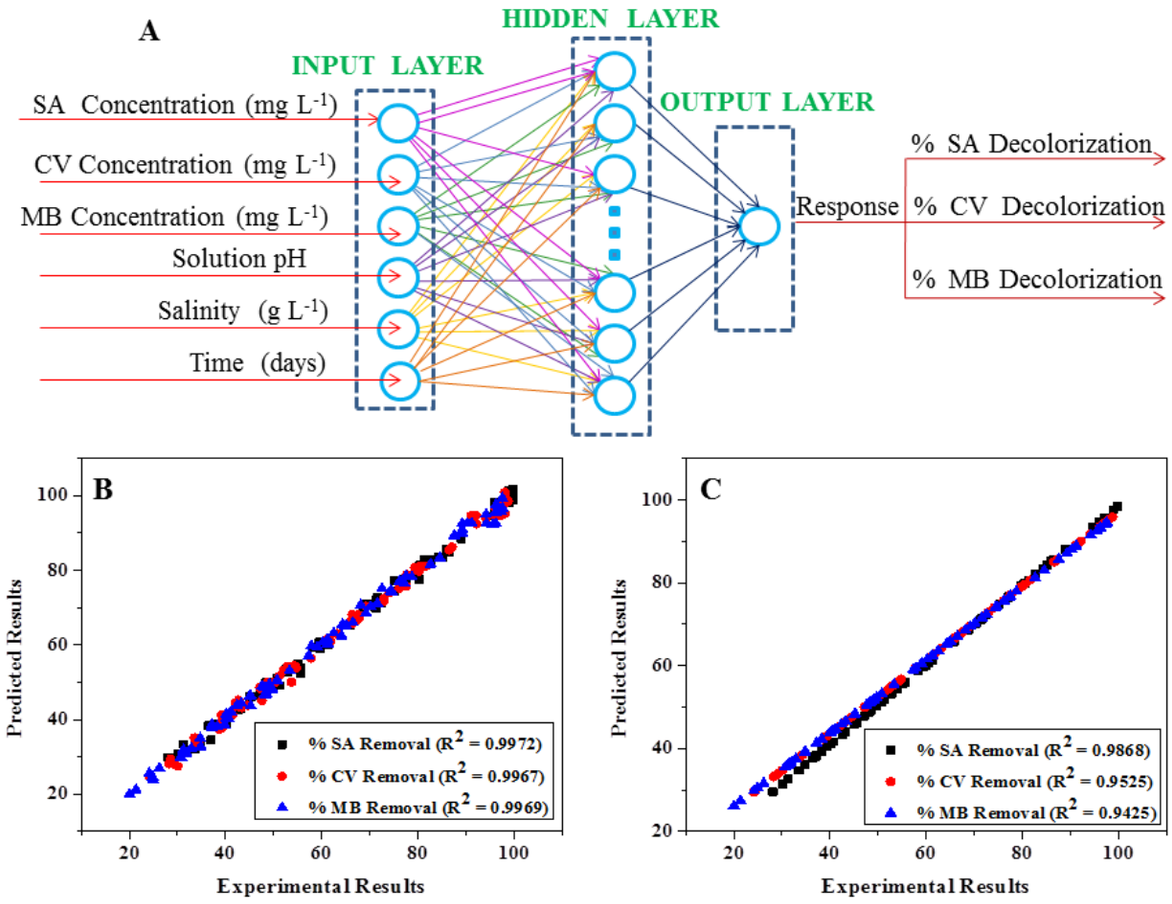

Fig. 4. Optimization and modeling of simultaneous SA, CV and MB degradation by selected bacterial consortium using RSM and ANN. (A) shows schematic architecture of developed back-propagation ANN model; (B and C) shows predicted removal (%) vs. experimental removal (%) of SA, CV and MB as obtained from RSM and ANN analysis respectively.

RSM predicted ones. Additionally the RSM model illustrated detailed description of interactions between linear, interaction and quadratic properties. RSM also significantly reduced the number of necessary experiments along with cost and time incurred and successfully optimized a complete quadratic model.

3.5. Atomic force microscopic analysis (AFM) of bacterial cells

Morphometric alterations of bacterial cells occurring as a result of exposure to ternary dye solutions have been visualized with AFM analysis. The tapping amplitude images of *Pseudomonas mendocina*, *Bacillus* sp. PD5 and *Dietzia* sp. PD1 have been illustrated in Fig. 5 (A–C) [in 2D] and (D–F) [in 3D] respectively prior to dye exposure and Fig. 5 (G–I) [in 2D] and (J–L) [in 3D] respectively post exposure. Morphological changes were estimated in terms of cell width, length and surface roughness (R_a). Cell length, width and surface roughness (R_a) were found to be 2.77 ± 0.031 µm, 994.21 ± 0.044 nm and 22.4 ± 0.026 nm respectively for *Pseudomonas mendocina* and 2.38 ± 0.017 µm, 474.76 ± 0.024 nm and 36.7 ± 0.018 nm correspondingly for *Dietzia* sp. prior to exposure to dye solutions. Post degradation studies, cells of *Pseudomonas mendocina* and *Dietzia* sp. attained a decreased cell length and width and an increase in surface roughness. The altered cell length, width and surface roughness (R_a) were found to be 1.64 ± 0.027 µm, 615.25 ± 0.036 nm and 313.82 ± 0.016 nm respectively for *Pseudomonas mendocina* and 1.35 ± 0.009 µm, 285.58 ± 0.04 nm and 411.67 ± 0.028 nm correspondingly for *Dietzia* sp. This may be attributed to the fact that *Pseudomonas mendocina* and *Dietzia* sp. PD1 were both Gram positive while *Bacillus* sp. PD5 was Gram negative in nature. Interaction between the thick peptidoglycan coating of Gram positive cells and dyes may be considered responsible for higher surface roughness of these bacterial species. Similar results were also reported by Nath and Ray [13] and Nikiyan et al. [27] in separate studies. On the other hand, Gram negative bacteria have highly reduced peptidoglycan coating rendering their outer membrane to possess flexible sensitivity towards detrimental compounds [27]. Hence, cells of gram negative *Bacillus* sp. PD5 was found to preserve its integrity (length 2.92 ± 0.039 µm, width 207.12 ± 0.016 nm and sur-

Table 1
Acute (24 h) and chronic (96 h) effects of different treatments [control (distilled water), untreated effluent (ternary dye solution containing 15 ppm of each of SA, CV and MB) and treated effluent (biotreated)] on growth, biochemical and stress responsive enzymatic parameters of root and shoot tissues of *Cicer arietinum* seedlings. All results are represented as Mean ± SD where $n = 25$. Statistically significant ($P < 0.05$) variations amidst different treatments for each type of tissue were indicated as: a, b. control vs. untreated effluent (for 24 h and 96 h exposure respectively), c, d. control vs. treated effluent (for 24 h and 96 h exposure respectively), e, f. untreated effluent vs. treated effluent (for 24 h and 96 h exposure respectively)

Alterations studied	Parameters assessed	Units	Treatments											
			In root						In shoot					
			Control		Untreated effluent		Treated effluent		Control		Untreated effluent		Treated effluent	
			After 24 h	After 96 h	After 24 h	After 96 h	After 24 h	After 96 h	After 24 h	After 96 h	After 24 h	After 96 h	After 24 h	After 96 h
Growth parameters	Length	Mm	3.28 ± 0.075a	7.14 ± 0.034b	1.33 ± 0.048	2.45 ± 0.082	3.05 ± 0.016e	6.84 ± 0.028f	2.37 ± 0.075a	6.18 ± 0.054b	0.87 ± 0.007	1.24 ± 0.032	2.12 ± 0.042e	5.87 ± 0.077f
Biochemical parameters	Protein content	mg mg^{-1} plant tissue	0.46 ± 0.035	0.42 ± 0.018	0.71 ± 0.051ae	0.83 ± 0.068bf	0.43 ± 0.004	0.48 ± 0.037	0.52 ± 0.012	0.57 ± 0.033	0.84 ± 0.057ae	0.92 ± 0.041bf	0.53 ± 0.005	0.54 ± 0.043
	Free amino acid content	mg mg^{-1} plant tissue	0.25 ± 0.015a	0.27 ± 0.009b	0.14 ± 0.011	0.06 ± 0.003	0.21 ± 0.008e	0.24 ± 0.031f	0.33 ± 0.027a	0.32 ± 0.055b	0.11 ± 0.009	0.02 ± 0.002	0.29 ± 0.047e	0.31 ± 0.022f
	Soluble carbohydrate content	mg mg^{-1} plant tissue	0.35 ± 0.015	0.38 ± 0.020	0.67 ± 0.038ae	0.72 ± 0.025bf	0.34 ± 0.044	0.36 ± 0.005	0.29 ± 0.013	0.32 ± 0.047	0.58 ± 0.028ae	0.67 ± 0.087bf	0.30 ± 0.017	0.33 ± 0.026
	Insoluble carbohydrate content	mg mg^{-1} plant tissue	0.72 ± 0.011a	0.75 ± 0.024e	0.48 ± 0.015	0.15 ± 0.007	0.73 ± 0.039b	0.77 ± 0.054f	0.92 ± 0.034a	0.96 ± 0.044b	0.42 ± 0.004	0.19 ± 0.006	0.88 ± 0.042e	0.91 ± 0.027f
	Amylase activity	mg maltose mg^{-1} protein h^{-1}	0.72 ± 0.031a	0.76 ± 0.046b	0.39 ± 0.022	0.27 ± 0.014	0.69 ± 0.027e	0.73 ± 0.035f	0.69 ± 0.051	0.73 ± 0.041a	0.23 ± 0.018b	0.12 ± 0.004	0.71 ± 0.104e	0.75 ± 0.094f
Oxidative stress response	POD activity	µmol min^{-1} mg^{-1} protein.	21.47 ± 2.21	24.36 ± 1.84	57.14 ± 0.87ae	66.25 ± 1.45bf	22.83 ± 0.06	23.57 ± 0.09	17.44 ± 1.24	19.56 ± 1.62	46.72 ± 2.25ae	52.43 ± 2.01bf	18.61 ± 0.72	20.37 ± 1.15
	CAT activity	µmol H_2O_2 consumed min^{-1} mg^{-1} protein	0.052 ± 0.002a	0.048 ± 0.005b	0.0024 ± 0.0007	0.0011 ± 0.0003	0.046 ± 0.004e	0.049 ± 0.0018f	0.064 ± 0.0024a	0.068 ± 0.0034b	0.0076 ± 0.0006	0.0051 ± 0.0004	0.059 ± 0.0018e	0.065 ± 0.0009f
	SOD activity	SOD units mg^{-1} protein	0.022 ± 0.0034	0.025 ± 0.0022	0.057 ± 0.0037ae	0.063 ± 0.0031bf	0.018 ± 0.0006	0.023 ± 0.0012	0.016 ± 0.0026	0.018 ± 0.0034	0.056 ± 0.0017ae	0.061 ± 0.0029bf	0.019 ± 0.0004	0.021 ± 0.0024
Detoxification response	GP_x activity	nmol NADPH oxidized min^{-1} mg^{-1}protein	0.132 ± 0.012a	0.127 ± 0.028b	0.074 ± 0.0049	0.062 ± 0.0063	0.128 ± 0.019e	0.130 ± 0.033f	0.118 ± 0.017a	0.122 ± 0.046b	0.067 ± 0.009	0.054 ± 0.0071	0.120 ± 0.057e	0.124 ± 0.021f
	GR activity	µmol of NADPH oxidized min^{-1} mg^{-1} protein	0.185 ± 0.003a	0.192 ± 0.014b	0.112 ± 0.021	0.087 ± 0.0086	0.178 ± 0.0057e	0.187 ± 0.018f	0.154 ± 0.019a	0.158 ± 0.037b	0.097 ± 0.0062	0.082 ± 0.0041	0.148 ± 0.004e	0.151 ± 0.016f
	GST activity	nmol CDNB conjugate formed $min^{-1}$$mg^{-1}$ protein	0.225 ± 0.019a	0.228 ± 0.024b	0.169 ± 0.047	0.127 ± 0.011	0.212 ± 0.074e	0.219 ± 0.058f	0.172 ± 0.034a	0.177 ± 0.067b	0.116 ± 0.027	0.094 ± 0.0064	0.167 ± 0.025e	0.174 ± 0.045f

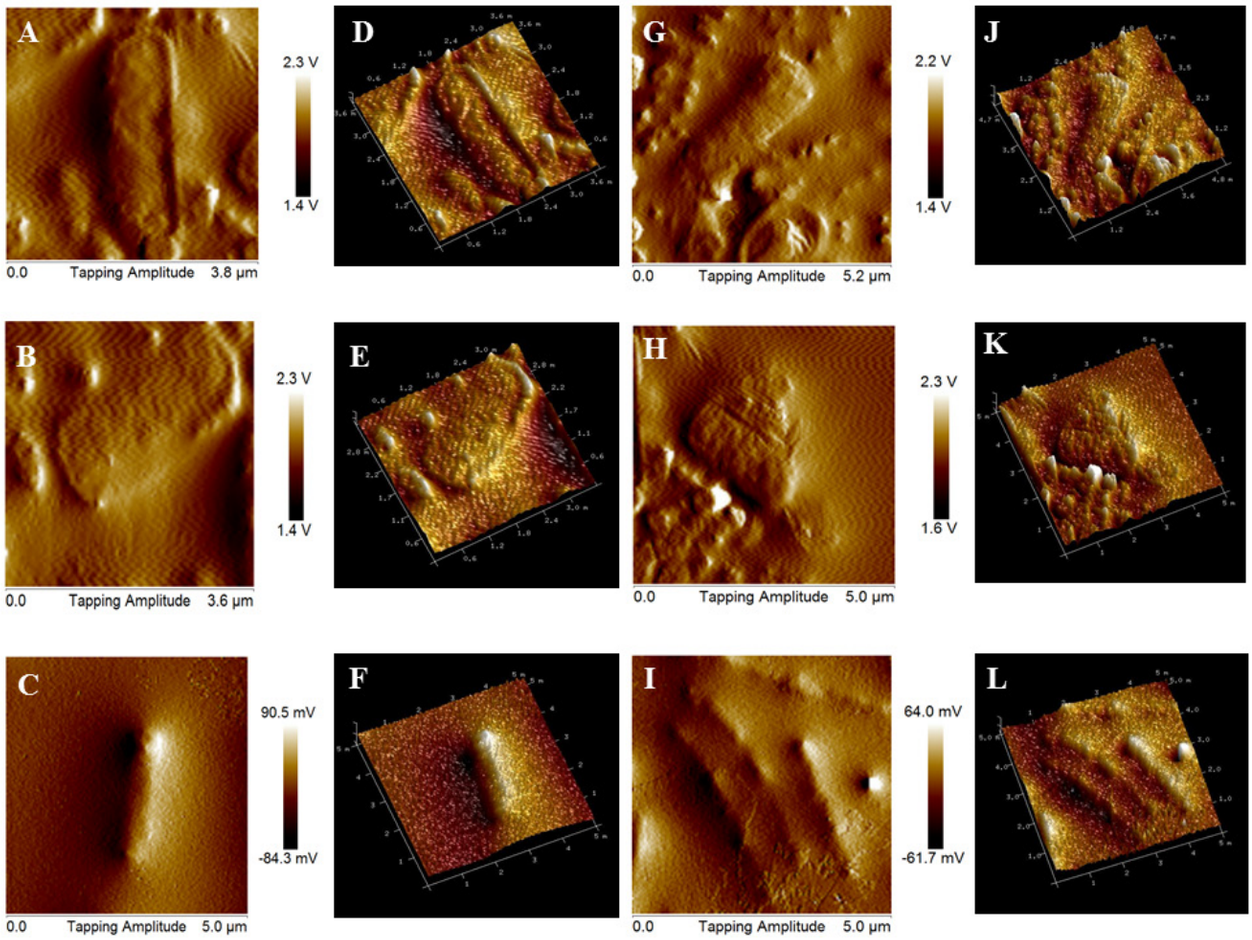

Fig. 5. Atomic force micrograph of *Pseudomonas mendocina, Bacillus* sp. and *Dietzia* sp. (A–C) show 2D and (D–F) show 3D images of *Pseudomonas mendocina, Bacillus* sp. and *Dietzia* sp respectively prior to dye exposure and (G–I) show 2D and (JL) show 3D images of *Pseudomonas mendocina, Bacillus* sp. and *Dietzia* sp respectively post exposure.

face roughness 27.8 ± 0.006 nm) on exposure to ternary dye solutions and undergo no significant change in surface roughness during the biodegradation studies.

3.6. FTIR Analysis of untreated and treated effluents

FTIR spectrum of untreated (spectrum A) and treated (spectrum B) ternary dye effluents have been shown in Fig. 6. Images of untreated and treated solutions have been provided in Fig. 6 (inset). Spectrum A displayed peaks at 3775, 3430, 2920, 1640, 1540 cm^{-1} corresponding to stretchings of –NH, $–NH_2$ (asymmetric), $–CH_3$ (asymmetric), –OH and carbonyl stretching respectively. Additionally two sharp peaks were recorded at 635 and 1260 cm^{-1} indicating that the dyes were of mono-substituted acetylene benzene derivative and aromatic nature [19]. Spectrum of the biodegraded product (spectrum B) yielded prominent peaks at 3441, 2940, 1685, 1457, 1361 representing –OH (weak), $–CH_3$, –OH stretching, $–CH_3$ bending (asymmetric), saturated C–H (strong) respectively [19,28]. Absence of peaks indicating carbonyl band and aromatic rings in spectrum B suggested successful degradation of dyestuff in effluent [28]. Other peaks present in spectrum B imply formation of oximes and imines as biodegraded products [19].

3.7. Phytotoxicity analysis

3.7.1. Effect on germination and growth

Germination in seeds is usually considered with the first emergence of radical in most plant species and may be impaired due to stress induced alterations of associated biochemical processes [29]. In this study, *Cicer arietinum* seeds were treated with control (distilled water), untreated (ternary dye solution bearing 15 mg L^{-1} of each dye) effluent and treated effluent (biodegraded effluent with selected bacterial consortium). Germination in all experimental groups was observed to initiate after an exposure period of 24 h. Seeds exposed to untreated effluent showed significant decrease in percentage germination ($p \leq 0.05$) in comparison to those exposed to treated effluent, which in turn were similar to con-

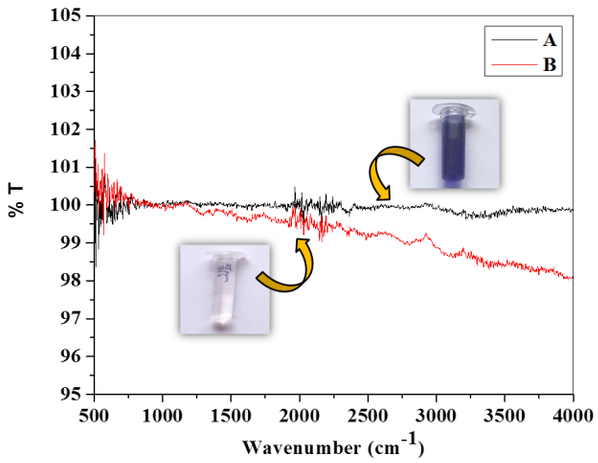

Fig. 6. FTIR spectrums of untreated (A) and treated; (B) effluents with visual representations of the effluents being shown inset.

trol treated ones. % germination of seeds recorded in control, untreated and treated seeds were found to be 76.15 ± 0.015, 18.11 ± 0.087 and 69.14 ± 0.022 respectively after an exposure of 24 h and further increased to 96.75 ± 0.027, 32.41 ± 0.064 and 94.85 ± 0.016 respectively at the end of 96 h. Additionally, growth of seedlings (recorded in terms of root and shoot length given in Table 1), was also found to be significantly higher in individuals exposed to control and treated effluents in comparison to those exposed to untreated effluents. Hence it may be concluded that biodegradation of ternary dyes efficiently curbed the toxic influences of ternary dye effluents lowering it to control levels.

3.7.2. Effect on biochemical parameters

Results of biochemical analysis of root and shoot tissues dissected out from experimental seedlings has been shown in Table 1. Individuals exposed to untreated effluents revealed significant ($p \leq 0.05$) increase in protein and insoluble carbohydrate content paralleled with a significant ($p \leq 0.05$) decrease in amino acid and soluble carbohydrate contents and amylase activity in a time dependent manner. However, values for these parameters were similar for seedlings exposed to control and treated effluents and any deviation recorded were insignificant. The variations in the protein and amino acid contents of seeds exposed to untreated effluents may have resulted from stress induced inhibition of proteolytic enzymes capable of degrading storage proteins in polypeptides and forming free amino acids. Inhibitions of these enzymes may further affect hormones and enzymes essential for the process of germination [22]. Amylase, a hydrolytic enzyme, is considered responsible for degradation of stored polysaccharides during seed germination [22]. Stress induced inhibition of amylase activity recorded in seedlings exposed to untreated effluent may have resulted in the increase and decrease observed respectively in soluble and insoluble carbohydrate contents of the same samples. Efficient detoxification of ternary dye effluent was established by the fact that similar biochemical profiles were obtained for seedlings exposed to both control and treated effluents.

3.7.3. Effect on oxidative stress response

Oxidative stress response in experimental seedlings was estimated in terms of POD, CAT and SOD activities as illustrated in Table 1. Peroxidases are oxido-reductase enzymes previously reported for catalysis of dehydrogenation of various organic compounds [21,22]. POD activity was determined to be significantly elevated ($p \leq 0.05$) in seedlings exposed to untreated effluents and further increased in a time dependent manner indicating an increased level of ROS formation. On the other hand, POD activity recorded in seedlings exposed to treated effluents were at par with that in control seedlings. SOD and CAT are two other enzymes reckoned for defending against oxidative stress by altering their activities accordingly [21]. A simultaneous time dependent and significant ($p \leq 0.05$) rise and fall of SOD and CAT activities respectively were recorded in seedlings exposed to untreated effluent in comparison to those exposed to untreated effluents, which in turn were similar to control levels. Elevated SOD levels suggested that a superoxide radical flux or stress induced inhibition of enzyme synthesis may be considered responsible for suppressed CAT activities.

GP_x, GR and GST participate in detoxification of oxidative stress occurring in organisms [10]. GPx is a selenium bearing enzyme that aids in combating oxidative damage by detoxifying SOD-generated hydrogen peroxide [10]. GST catalyzes metabolism of various electrophilic compounds while GR prevent peroxide attack on cell membranes by maintaining reduced Glutathione (GSH) levels of the cell. Results obtained in this study showed a significant time dependent decrease ($p \leq 0.05$) in all three detoxification enzyme activities in tissues obtained from seedlings exposed to untreated effluents. GP_x, GR and GST cumulatively execute detoxification of stress inducing compounds and thereby prevent probable DNA damage [10]. Suppression of these enzyme activities indicated irreparable damage of plant detoxification mechanism resulting from exposure to untreated effluent. Detoxification enzyme activities recorded in seedlings exposed to treated effluent remained constant with time and neared control levels indicating efficient detoxification of ternary dye system using selected bacterial consortium.

4. Conclusion

The present study is the first report of optimization and modeling of simultaneous bacterial degradation of three azine dyes and therefore has significant implications for wide scale implementation of bioremediation technology in treatment of real time industrial wastewater rich in mixed dyes and high salt concentrations. RSM optimization and ANN modeling proved to be vital tools for achieving excellent process optimization with highly reduced cost and time. The bacterial strains utilized in this study are capable of complete detoxification of mixed dye solutions as evident from the FTIR analysis and phytotoxicity assay conducted with the untreated and treated effluents on a comparative scale. Results of the phytotoxicity assay also confirmed the benign nature of biotreated water rendering it safe for discharge or reuse in agricultural processes. Cell surface study of bacterial cells (performed with AFM) hereby established the higher potentials of Gram –ve bacteria for dye degradation over Gram +ve strains. Hence, it may be concluded that

the microbial consortium selected in this study performed highly efficient treatment of wastewater in terms of both qualitative and quantitative parameters thereby suggesting the possibility of successful administration of bioremediation for real time effluents rich in mixed pollutants.

Conflicts of interest

Authors declare that they have no conflict of interest.

Acknowledgement

The authors are thankful to all members of Department of Environmental Science, University of Calcutta and Department of Chemical Engineering, Jadavpur University. Authors also acknowledge Mr. Sourav Chakraborty, DBT-Interdisciplinary Program in Life Sciences, University of Calcutta, and Mr. Sudipto Goswami, Department of Chemical Engineering, Jadavpur University for helping us with the AFM and FTIR analyses respectively.

Funding: This work was supported by the Department of Biotechnology, Government of West Bengal (Grant Number 348/BT (Estt.) /RD-10/2013).

References

[1] P. Das, P. Banerjee, S. Mondal, Mathematical modelling and optimization of synthetic textile dye removal using soil composites as highly competent liner material, Environ. Sci. Poll. Res., 22 (2015) 1318–1328.

[2] P. Banerjee, S. Sau, P. Das, A. Mukhopadhayay, Optimization and modelling of synthetic azo dye waste water treatment using graphene oxide nanoplatelets: Characterization toxicity evaluation and optimization using artificial neural network, Ecotoxicol. Environ. Saf., 119 (2015) 47–57.

[3] T.A. Khan, S. Dahiya, I. Ali, Removal of direct red 81 dye from aqueous solution by native and citric acid modified bamboo saw dust- kinetic study and equilibrium isotherm analyses, Gazi Univ. J. Sci., 25 (2012) 59–87.

[4] A. Santos, S. Mendes, V. Brissos, L.O. Martins, New dye-decolorizing peroxidases from *Bacillus subtilis* and *Pseudomonas putida* MET94: towards biotechnological applications, Appl. Microbiol. Biotechnol., 98 (2013) 2053–2065.

[5] N.O. San, A. Celebioglu, Y. Tümtas, T. Uyar, T. Tekinay, Reusable bacteria immobilized electrospun nanofibrous webs for decolorization of methylene blue dye in wastewater treatment, R.S.C. Adv., 4 (2014) 32249–32255.

[6] K.I. Karapinar, F. Karagi, G. Mcmullan, R. Marchan, Decolorization of textile dyestuffs by a mixed bacterial consortium, Biotechnol. Lett., 22 (2000) 1179–1189.

[7] M. Cerboneschi, M. Corsi, R. Bianchini, M. Bonanni, S. Tegli, Decolorization of acid and basic dyes: understanding the metabolic degradation and cell-induced adsorption/precipitation by Escherichia coli, Appl. Microbiol. Biotechnol., 99 (2015) 8235–8245.

[8] R. Mahmood, F. Sharif, S. Ali, M.U. Hayyat, Enhancing the decolorizing and degradation ability of bacterial consortium isolated from textile effluent affected area and its application on seed germination, The Sci. World J., (2015) Doi: 10.1155/2015/628195.

[9] R.G. Saratale, G.D. Saratale, D.C. Kalyani, J.S. Chang, S.P. Govindwar, Enhanced decolorization and biodegradation of textile azo dye Scarlet R by using developed microbial consortium-GR. Biores, Technol., 100 (2009), 2493–2500.

[10] P. Banerjee, S. Sarkar, T.K. Dey, M. Bakshi, S. Swarnakar, A. Mukhopadhyay, S. Ghosh, Application of isolated bacterial consortium in UMBR for detoxification of textile effluent: Comparative analysis of resultant oxidative stress and genotoxicity in catfish (*Heteropneustes fossilis*) exposed to raw and treated effluents, Ecotoxicology 23 (2014) 1073–1085.

[11] P. Das, P. Banerjee, A. Zaman, P. Bhattacharya, Biodegradation of two Azo dyes using *Dietzia* sp. PD1: process optimization using response surface methodology and artificial neural network, Desal. Water Treat., 57 (2016) 7293–7301.

[12] S. Sarnaik, P. Kanekar, Biodegradation of methyl violet by Pseudomonas mendocina MCM B-402, Appl. Microbiol. Biotechnol., 52 (1999) 251–254.

[13] J. Nath, L. Ray, Biosorption of Malachite green from aqueous solution by dry cells of Bacillus cereus M116 (MTCC 5521), J. Environ. Chem. Eng., 3 (2015) 386–394.

[14] B.D. Tony, D. Goyal, S. Khanna, Decolorization of textile azo dyes by aerobic bacterial consortium, Int. Biodeter. Biodeg., 63 (2009) 462–469.

[15] G. Derringer, R. Suich, Simultaneous optimization of several response variables, J. Qua. Technol., 12 (1980) 214–219.

[16] K. Sinha, P.D. Saha, S. Datta, Response surface optimization and artificial neural network modelling of microwave assisted natural dye extraction from pomegranate rind. Indus, Crops Prod., 37 (2012) 408–414.

[17] S. Dutta, S.A. Parsons, C. Bhattacharjee, S. Bandhyopadhyay, S. Datta, Development of an artificial neural network model for adsorption and photocatalysis of reactive dye on TiO_2 surface, Expert Syst. Appl., 37 (2010) 8634–8638.

[18] F.N. Azad, M. Ghaedi, A. Asfaram, A. Jamshidi, G. Hassani, A. Goudarzi, M.H.A. Azqhandi, A.M. Ghaedi, Optimization of the process parameters for the adsorption of ternary dyes by Ni doped FeO (OH)-NWs-AC using response surface methodology and artificial neural network, R.S.C. Adv., 6 (2016) 19768–19779.

[19] D.C. Kalyani, P.S. Patil, J.P. Jadhav, S.P. Govindwar, Biodegradation of reactive textile dye Red BLI by an isolated bacterium Pseudomonas sp. SUK1. Biores. Technol., 99 (2008) 4635–4641.

[20] S. Keshavkant, J. Padhan, S. Parkhey, S.C. Naithani, Physiological and antioxidant responses of germinating Cicer arietinum seeds to salt stress, Russian J. Plant Physiol., 59 (2012) 206–211.

[21] P. Banerjee, M. Satapathy, A. Mukhopahayay, P. Das, Leaf extract mediated green synthesis of silver nanoparticles from widely available Indian plants: synthesis, characterization, antimicrobial property and toxicity analysis, Biores. Bioproc., (2014) Doi: 10.1186/s40643-014-0003-y.

[22] M.R. Goswami, P. Banerjee, S. Swarnakar, A. Mukhopadhyay, Carbaryl mediated biochemical alterations in Eggplant (Solanum melongena L.), Int. J. Environ. Sci. Technol., 3 (2013), 51–57.

[23] Z.W. Wang, J.S. Liang, Y. Liang, Decolorization of Reactive Black 5 by a newly isolated bacterium *Bacillus* sp. YZU1, Int. Biodeter. Biodeg., 76 (2013) 41–48.

[24] K. Rajeswari, R. Subashkumar, K. Vijayaraman, Decolorization and degradation of textile dyes by *Stenotrophomonas maltophilia* RSV-2, Int. J. Environ. Biorem. Biodeg., 1 (2013) 60–65.

[25] S. Asad, M.A. Amoozegar, A.A. Pourbabaee, M.N. Sarbolouki, S.M.M. Dastgheib, Decolorization of textile azo dyes by newly isolated halophilic and halotolerant bacteria, Biores. Technol., 98 (2007) 2082–2088.

[26] Y.M. Kolekar, S.P. Pawar, K.R. Gawai, P.D. Lokhande, Y.S. Shouche, K.M. Kodam, Decolorization and degradation of Disperse Blue 79 and Acid Orange 10, by *Bacillus fusiformis* KMK5 isolated from the textile dye contaminated soil, Biores. Technol., 99 (2008) 8999–9003.

[27] H. Nikiyan, A. Vasilchenko, D. Deryabin, AFM investigations of various disturbing factors on bacterial cells, in: A., Méndez-Vilas, J.Díaz, (Eds.), Microscopy: Science, Technology, Applications and Education, Formatex Research Center, Spain, 2010 pp. 523–529.

[28] Y. Li., D.L. Xi, Decolorization and biodegradation of dye wastewaters by facultative-aerobic process, Environ. Sci. Poll. Res., 11 (2004) 372–377.

[29] P. Bhattacharya, K. Mallick, S. Ghosh, P. Banerjee, A. Mukhopadhyay, S. Bandyopadhyay, Algal biomass as potential biosorbent for reduction of organic load in gray water and subsequent reuse: Effect on seed germination and enzyme activity, Biorem. J., 18 (2014) 56–70.

Supplementary Materials

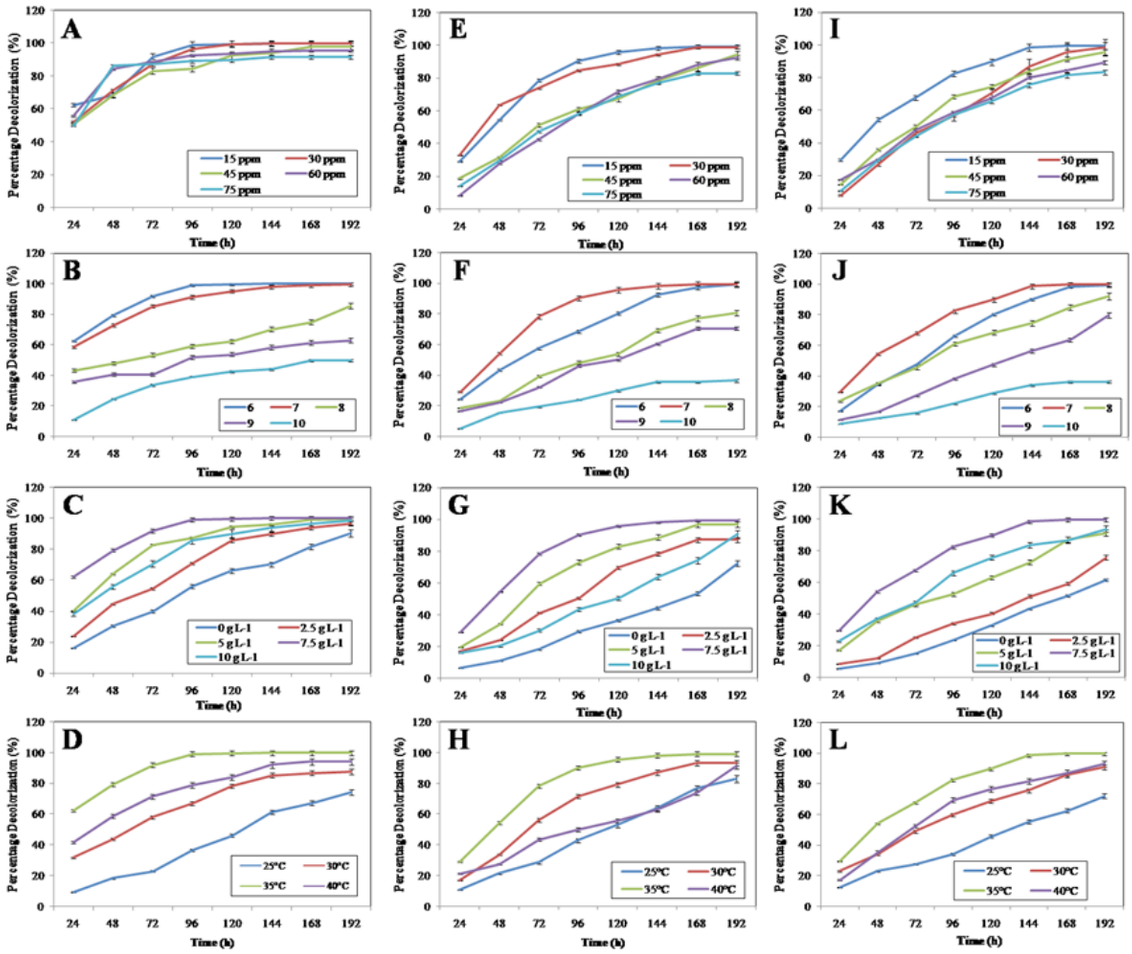

SF. 1. Effect of experimental parameters on the simultaneous SA, CV and MB degradation by selected bacterial consortium. Fig. A–D, E–H and I–L show effect of different initial dye concentration, variable pH, salt concentration and temperature with respect to duration of treatment on SA, CV and MB % decolorization respectively. Other parameters were kept constant throughout the experiment. Bars indicate SD.

Table 1
Comparative analysis of results obtained from RSM optimization (with computational details of CCD) and ANN modeling for simultaneous SA, CV and MB removal using selected bacterial consortium

Details of response surface methodology (CCD) optimization							Comparative analysis of RSM and ANN approach						
Factors	Units	Levels		Star point α = 2.00			Statistical parameters	Models					
		Low (–1)	Central (0)	High (+1)	–α	+α		RSM			ANN		
								SA	CV	MB	SA	CV	MB
A: SA Conc.	mg L^{-1}	6.63	12.50	18.37	0.76	24.24							
B: CV Conc.	mg L^{-1}	6.63	12.50	18.37	0.76	24.24							
C: MB Conc.	mg L^{-1}	6.63	12.50	18.37	0.76	24.24	R^2	0.9972	0.9967	0.9969	0.9868	0.9525	0.9425
D: pH		3.3	6.3	9.3	2.3	12.3	RMSE	1.198	1.268	1.332	0.924	2.703	3.109
E: Salinity	g L^{-1}	5.54	7.50	9.46	3.59	11.41	MAE	0.0006	0.034	0.023	0.183	0.787	1.133
F: Time	days	4	7	10	2	13	AAD%	0.019	0.099	0.008	0.212	2.828	3.909

Run	Recommended Factors						% SA Removal			% CV Removal			% MB Removal		
	A	B	C	D	E	F	Predicted		Experimental	Predicted		Experimental	Predicted		Experimental
							RSM	ANN		RSM	ANN		RSM	ANN	
1	18.37	6.63	18.37	3.3	9.46	4	32.07	34.80	33.54	30.52	34.75	30.06	23.76	30.55	24.94
2	18.37	6.63	6.63	3.3	9.46	10	52.29	56.00	55.62	50.05	55.80	53.71	48.50	51.14	48.34
3	6.63	18.37	18.37	9.3	9.46	10	99.56	98.48	99.87	98.52	95.88	98.74	95.81	94.26	97.34
4	6.63	18.37	6.63	9.3	9.46	4	83.61	84.32	85.12	79.80	79.40	80.23	76.55	76.52	77.18
5	6.63	18.37	6.63	9.3	5.54	10	82.84	80.62	81.27	80.79	78.68	79.42	77.07	75.64	76.18
6	12.50	12.50	12.50	6.3	7.50	7	98.12	94.64	95.87	94.71	89.10	91.12	92.60	88.84	91.18
7	6.63	18.37	18.37	3.3	5.54	4	48.21	48.74	48.06	43.19	46.55	43.32	40.36	44.34	40.61
8	6.63	6.63	18.37	9.3	9.46	4	74.41	74.74	75.15	70.41	69.54	69.15	66.05	67.09	66.47
9	6.63	18.37	18.37	3.3	5.54	10	55.08	55.53	55.14	49.89	52.62	50.14	46.90	51.29	48.51
10	6.63	18.37	18.37	3.3	9.46	4	42.75	43.52	42.62	39.40	42.85	39.16	35.03	39.15	34.72
11	0.76	12.50	12.50	6.3	7.50	7	70.55	68.72	68.87	66.37	66.86	66.13	60.76	61.61	60.24
12	18.37	18.37	6.63	3.3	9.46	10	46.40	47.84	47.12	41.69	44.79	41.34	38.13	42.27	38.26
13	12.50	12.50	12.50	6.3	11.41	7	70.84	68.52	68.67	68.18	67.14	66.45	65.49	65.20	64.32
14	12.50	12.50	12.50	2.3	7.50	7	46.27	46.33	45.55	41.26	42.85	39.16	37.92	41.35	37.22
15	18.37	18.37	6.63	9.3	9.46	10	99.97	98.48	99.87	96.63	93.54	96.11	94.99	91.46	94.16
16	18.37	18.37	6.63	3.3	5.54	4	29.81	29.60	28.12	24.29	29.87	24.57	20.00	26.22	20.02
17	12.50	12.50	12.50	6.3	3.59	7	60.15	61.37	61.22	56.49	59.36	57.71	53.14	55.53	53.33
18	18.37	6.63	18.37	9.3	9.46	10	96.03	95.71	96.99	94.01	91.78	94.13	90.02	87.13	89.24
19	18.37	6.63	6.63	9.3	9.46	4	77.16	76.51	76.99	72.48	72.85	72.87	70.27	70.31	70.12
20	18.37	18.37	6.63	3.3	9.46	4	30.81	31.52	30.12	24.62	29.51	24.17	21.22	27.44	21.41
21	12.50	12.50	12.50	6.3	7.50	7	98.12	94.75	95.99	94.71	89.11	91.13	92.60	87.13	89.24

(Continued)

Table 1 *(Continued)*

Run	Recommended Factors						% SA Removal			% CV Removal			% MB Removal		
	A	B	C	D	E	F	Predicted		Experimental	Predicted		Experimental	Predicted		Experimental
							RSM	ANN		RSM	ANN		RSM	ANN	
22	18.37	6.63	6.63	3.3	9.46	4	33.29	32.63	31.28	29.47	33.47	28.62	27.00	31.69	26.24
23	18.37	18.37	18.37	3.3	5.54	10	46.12	45.92	45.12	41.22	44.86	41.42	38.62	43.69	39.87
24	18.37	18.37	18.37	9.3	9.46	10	98.69	98.48	99.87	95.26	95.31	98.10	92.26	92.70	95.57
25	12.50	12.50	12.50	6.3	7.50	2	69.88	70.96	71.21	61.98	62.72	61.48	59.73	59.53	57.88
26	6.63	6.63	18.37	9.3	9.46	10	94.52	93.55	94.74	92.47	89.97	92.10	89.35	85.66	87.57
27	24.24	12.50	12.50	6.3	7.50	7	59.08	59.87	59.66	54.39	56.17	54.12	48.64	51.00	48.18
28	18.37	18.37	18.37	9.3	9.46	4	77.34	74.80	75.21	70.40	69.56	69.17	65.12	65.70	64.89
29	6.63	18.37	6.63	3.3	5.54	10	49.58	50.35	49.74	44.58	45.49	42.12	38.70	41.32	37.18
30	12.50	12.50	12.50	12.3	7.50	7	72.02	70.99	71.24	67.34	68.31	67.76	63.19	63.63	62.53
31	18.37	18.37	18.37	3.3	5.54	4	34.60	38.16	37.04	28.21	33.93	29.13	25.66	29.87	24.17
32	12.50	0.76	12.50	6.3	7.50	7	100.3	98.48	99.87	98.93	95.61	98.44	96.42	94.10	97.16
33	18.37	18.37	6.63	9.3	5.54	10	77.62	79.71	80.32	75.18	75.77	76.15	71.16	71.57	71.56
34	6.63	6.63	6.63	3.3	9.46	4	38.93	41.23	40.24	34.38	38.09	33.81	31.30	36.42	31.61
35	18.37	6.63	18.37	9.3	5.54	4	60.77	59.76	59.54	54.44	56.29	54.26	49.48	51.84	49.14
36	6.63	18.37	18.37	9.3	5.54	4	71.13	70.32	70.54	66.62	67.86	67.26	62.39	65.04	64.14
37	12.50	12.50	12.50	6.3	7.50	7	98.12	97.63	98.99	94.71	90.00	92.13	92.60	88.01	90.24
38	6.63	6.63	6.63	3.3	9.46	10	53.28	53.13	52.64	48.65	49.98	47.17	44.38	46.66	43.25
39	18.37	18.37	18.37	3.3	9.46	10	49.79	49.04	48.37	45.23	45.99	42.69	42.13	44.80	41.14
40	18.37	6.63	18.37	3.3	5.54	10	53.69	53.23	52.74	49.99	51.26	48.61	46.53	48.36	45.18
41	6.63	6.63	18.37	3.3	5.54	4	49.99	49.18	48.52	43.66	45.54	42.18	41.45	43.95	40.17
42	18.37	6.63	18.37	9.3	9.46	4	71.27	72.15	72.45	65.63	66.86	66.14	60.30	62.57	61.33
43	6.63	18.37	18.37	3.3	9.46	10	53.78	56.01	55.64	50.08	52.71	50.24	46.15	48.30	45.11
44	6.63	6.63	6.63	3.3	5.54	10	59.29	58.67	58.41	54.12	56.60	54.61	49.00	50.51	47.62
45	6.63	18.37	6.63	9.3	9.46	10	100.2	98.48	99.87	98.43	95.31	98.10	96.63	94.46	97.57
46	12.50	12.50	12.50	6.3	7.50	7	98.12	97.63	98.99	94.71	93.56	96.13	92.60	91.53	94.24
47	6.63	6.63	6.63	9.3	9.46	10	99.70	98.48	99.87	97.94	95.31	98.10	96.79	94.46	97.57
48	12.50	12.50	12.50	6.3	7.50	7	98.12	97.63	98.99	94.71	93.56	96.13	92.60	88.89	91.24
49	6.63	18.37	18.37	9.3	5.54	10	83.66	83.50	84.27	81.19	79.57	80.42	78.53	76.81	77.51
50	18.37	18.37	6.63	3.3	5.54	10	41.25	41.71	40.74	37.37	42.36	38.61	32.34	37.53	32.87
51	12.50	12.50	12.50	6.3	7.50	7	98.12	97.63	98.99	94.71	93.56	96.13	92.60	88.89	91.24
52	6.63	18.37	6.63	3.3	9.46	10	49.77	51.21	50.64	45.08	50.31	47.54	40.23	44.02	40.25
53	6.63	18.37	6.63	9.3	5.54	4	70.39	70.23	70.45	66.15	66.57	65.81	61.56	62.47	61.22
54	6.63	18.37	6.63	3.3	5.54	4	42.80	44.01	43.14	37.81	42.97	39.29	32.79	39.29	34.87
55	6.63	6.63	6.63	9.3	9.46	4	79.68	79.52	80.12	75.80	77.04	77.57	74.12	74.29	74.65

56	6.63	6.63	18.37	3.3	5.54	10	60.27	61.44	61.29	53.87	56.72	54.74	50.57	53.27	50.76
57	18.37	6.63	6.63	9.3	5.54	4	65.17	65.79	65.82	60.99	62.97	61.76	57.17	59.03	57.31
58	18.37	6.63	18.37	9.3	5.54	10	81.37	79.80	80.42	78.84	77.14	77.68	74.63	74.05	74.37
59	18.37	18.37	18.37	9.3	5.54	10	77.83	76.92	77.42	74.11	73.97	74.12	70.71	68.55	68.12
60	18.37	18.37	18.37	3.3	9.46	4	34.11	36.06	34.85	28.24	33.18	28.29	24.59	30.46	24.84
61	6.63	6.63	18.37	3.3	9.46	10	52.77	53.33	52.84	48.09	51.77	49.18	43.67	48.41	45.24
62	6.63	6.63	6.63	9.3	5.54	4	72.66	71.37	71.64	68.13	68.14	67.57	65.27	65.86	65.07
63	18.37	6.63	6.63	9.3	5.54	10	85.68	85.10	85.94	85.46	85.03	86.55	81.69	81.32	82.64
64	12.50	12.50	12.50	6.3	7.50	13	101.42	97.63	98.99	97.13	94.45	97.13	95.36	93.29	96.24
65	18.37	18.37	18.37	9.3	5.54	4	60.64	60.62	60.44	53.24	54.41	52.15	48.15	52.38	49.75
66	12.50	24.24	12.50	6.3	7.50	7	96.66	94.75	95.99	94.15	91.78	94.13	90.95	87.13	89.24
67	6.63	6.63	18.37	9.3	5.54	10	84.82	85.68	86.54	81.12	80.64	81.62	78.22	77.92	78.77
68	18.37	6.63	18.37	3.3	9.46	10	51.16	51.24	50.67	48.03	50.26	47.48	43.88	45.90	42.39
69	6.63	18.37	18.37	9.3	9.46	4	82.87	82.04	82.75	79.97	79.13	79.92	75.10	72.44	72.54
70	12.50	12.50	12.50	6.3	7.50	7	98.12	97.63	98.99	94.71	93.56	96.13	92.60	91.53	94.24
71	18.37	18.37	6.63	9.3	9.46	4	78.71	79.25	79.84	71.69	72.90	72.92	68.48	69.50	69.21
72	6.63	6.63	18.37	3.3	9.46	4	38.33	37.59	36.45	33.89	38.09	33.81	29.97	35.56	30.64
73	6.63	6.63	18.37	9.3	5.54	4	68.87	68.49	68.64	63.04	64.19	63.14	59.49	60.58	59.07
74	12.50	12.50	24.24	6.3	7.50	7	99.35	97.63	98.99	96.61	94.45	97.13	95.84	93.29	96.24
75	12.50	12.50	0.76	6.3	7.50	7	99.74	97.63	98.99	98.16	94.45	97.13	97.62	93.29	96.24
76	6.63	6.63	6.63	3.3	5.54	4	49.11	51.72	51.17	43.84	47.67	44.57	40.50	44.02	40.25
77	18.37	6.63	18.37	3.3	5.54	4	38.76	40.40	39.37	33.47	38.43	34.19	30.98	36.71	31.94
78	12.50	12.50	12.50	6.3	7.50	7	98.12	97.63	98.99	94.71	93.56	96.13	92.60	91.53	94.24
79	18.37	6.63	6.63	3.3	5.54	4	38.50	38.28	37.17	35.11	37.88	33.57	31.94	36.10	31.25
80	6.63	6.63	6.63	9.3	5.54	10	88.52	88.03	88.99	86.29	85.52	87.10	83.37	83.02	84.57
81	6.63	18.37	6.63	3.3	9.46	4	38.83	39.38	38.31	34.32	38.59	34.37	29.75	35.77	30.87
82	18.37	6.63	6.63	9.3	9.46	10	101.83	98.35	99.74	100.9	95.31	98.10	99.37	94.46	97.57
83	12.50	12.50	12.50	6.3	7.50	7	98.12	97.63	98.99	94.71	94.45	97.13	92.60	93.29	96.24
84	18.37	6.63	6.63	3.3	5.54	10	53.34	54.41	53.97	51.71	53.58	51.21	46.86	50.95	48.12
85	12.50	12.50	12.50	6.3	7.50	7	98.12	97.63	98.99	94.71	94.45	97.13	92.60	93.29	96.24
86	18.37	18.37	6.63	9.3	5.54	4	60.52	60.08	59.87	54.22	55.12	52.94	49.23	51.83	49.12